CORE
Metadata, citation and similar papers at core.ac.uk
Provided by Queensland University of Technology ePrints Archive

Queensland University of Technology
Brisbane Australia

This is the author's version of a work that was submitted/accepted for publication in the following source:

Rusthi, Mohamed, Keerthan, Poologanathan, Mahendran, Mahen, & Ariyanayagam, Anthony
(2017)
Investigating the fire performance of LSF wall systems using finite element analyses.
Journal of Structural Fire Engineering.

This file was downloaded from: https://eprints.qut.edu.au/109437/

© **Emerald Publishing Limited 2017**

Notice: *Changes introduced as a result of publishing processes such as copy-editing and formatting may not be reflected in this document. For a definitive version of this work, please refer to the published source:*

https://doi.org/10.1108/JSFE-04-2016-0002

Investigating the Fire Performance of LSF Wall Systems using Finite Element Analyses

Mohamed Rusthi [a], Poologanathan Keerthan [a], **Mahen Mahendran** [a,*] and Anthony Ariyanayagam [a]

[a] *Queensland University of Technology (QUT), Brisbane, QLD 4000, Australia*

[*] *Corresponding author's email address:* m.mahendran@qut.edu.au

Abstract

This research was focused on investigating the fire performance of LSF wall systems by using 3-D heat transfer finite element models of existing LSF wall system configurations. The analysis results were validated by using the available fire test results of five different LSF wall configurations. The validated finite element models were then used to conduct a parametric study on a range of non-load bearing and load bearing LSF wall configurations to predict their fire resistance levels (FRLs) for varying load ratios. The fundamental understanding of the fire performance of LSF wall systems was improved by using the validated 3-D finite element models and the parametric study predictions. Using the 3-D finite element models developed in this research, a fully-coupled finite element modelling approach can be developed to investigate the thermal-mechanical behaviour of LSF wall systems simultaneously. This paper presents the details of this research and the results.

Keywords: Fire performance, Finite element analysis, Heat transfer analysis, Light-gauge steel frame wall systems

Total words: 6886

1 INTRODUCTION

Cold-formed light-gauge steel frame (LSF) wall frame systems are widely adopted in contemporary buildings due to higher strength-to-weight ratio, improved durability, enhanced thermal comfort, light-weight, aesthetic appearance, and cost effectiveness compared to hot-rolled steel frame systems. Fire resistance of LSF wall systems is an important factor in preventing the spread of fire and eventually the building collapse due to strength degradation of cold-formed steel at elevated temperatures. This can be achieved by having single or multiple layers of fire protective wall boards on both sides of the LSF wall to prevent the steel studs from being heated to failure temperatures.

Fire performance of LSF wall systems with different configurations can be understood by performing full-scale fire tests. Many experimental research studies [1-4] have been conducted on various LSF wall configurations exposed to fire. However, these full-scale fire tests are time consuming, labour intensive and expensive. On the other hand, finite element analysis (FEA) provides a simple method of investigating the fire performance of LSF wall systems to understand their thermal-mechanical behaviour. Recent numerical research studies [5-9] have focused on investigating the fire performances of LSF wall systems by using finite element (FE) models. Most of these FE models were developed based on 2-D FE platform capable of performing either heat transfer or structural analysis separately. There is a need to develop the capabilities to perform fully coupled thermal-mechanical analyses of LSF walls exposed to fire, for which a 3-D FE modelling approach can be used.

This research was aimed at investigating the fire performance of LSF wall systems by using 3-D heat transfer FE models of existing LSF wall system configurations. The analysis results were validated using the fire test results of five load bearing LSF wall configurations. The validated FE models were then used to conduct a series of parametric studies on the existing and innovative non-load bearing and load bearing LSF wall configurations to predict their fire resistance levels (FRLs) at varying load ratios. The FRLs of LSF wall systems are stated based on the time limits defined by three criteria given in AS 1530.4 [10]. They are: 1) structural: wall must continue to carry the design loads, 2) integrity: wall's integrity is not affected to allow the penetration of hot gases or flames and 3) insulation: wall's insulation to restrict heat passing thorough the wall (i.e., the ambient or unexposed surface wall temperature should not exceed 160 ºC on average or 200 ºC at any point when the assumed room temperature is 20 ºC).

The fundamental understanding of the thermal performance of LSF wall systems was improved by the predictions obtained from the parametric studies based on the validated 3-D FE models discussed in the paper. This paper presents the details of this research and its results. It also includes a brief literature review of the FE modelling approaches used in the past and the findings.

2 LITERATURE REVIEW

Recently, researchers have mainly focused on understanding the fire behaviour of different LSF wall system configurations while incorporating new strategies to improve the fire performance (i.e. increase FRLs). These strategies were experimentally and numerically evaluated by incorporating different stud sections [1,11], adding more plasterboard layers [12], changing the type of wall boards other than conventionally used gypsum plasterboards such as MgO boards and calcium silicate boards[3,4], using enhanced plasterboards by additives and fillers [13], including external or sandwiched insulation between two plasterboards [14], including different insulation materials with varying thickness and materials such as rock, glass, and cellulose fibre insulation materials [2,15] and evaluating the difference between realistic and standard fire curves [16].

Valuable data from experimental studies of LSF walls are used to calibrate numerical models. Such calibrated numerical models can be used to perform parametric analyses by changing the configurations of LSF walls. This will enable better understanding of the research problem. Three different types of thermal-mechanical modelling are available in the finite element software, which are [17];

- Uncoupled thermal modelling: Used when only the heat transfer through elements needs to be evaluated.
- Sequentially coupled thermal-mechanical modelling: Used when mechanical performance of a structure depends on the temperature field. Initially, uncoupled thermal modelling is performed and then the temperature results from this analysis will be transferred into a mechanical model to conduct separate mechanical analysis.
- Fully coupled thermal-mechanical modelling: Used when both mechanical and thermal solutions depend on each other and the results need to be acquired at the same time.

A range of finite element modelling and analysis software is currently available. In recent research studies, SAFIR and Abaqus have been extensively used and are the most commonly used FE software used in investigating the thermal performance of LSF wall systems. SAFIR has been extensively used to simulate fire test results [5-9]. However, these analyses were limited to 2-D models of LSF wall systems. Therefore, the use of Abaqus as an alternative in 2-D and 3-D thermal-mechanical modelling is discussed next.

Feng et al. [18] performed experiments on cold-formed steel wall panel systems with and without cavity insulation exposed to standard fire. Their test results were compared with the analysis results from Abaqus. Finite element analyses of different steel panel system configurations were conducted using 2-D FE models to understand the effect of different modelling parameters such as thermal boundary conditions and material properties. Convection and radiation effects were the thermal boundary conditions considered in their analyses. On the external surfaces of the steel panel systems, radiation and convection boundary conditions were adopted. Emissivity values for fire exposed and ambient side surfaces were assigned as 0.0 and 0.8, respectively, whereas the convection heat transfer coefficients were 25 $W/m^2/^oC$ on the fire exposed surface and 10 $W/m^2/^oC$ on the ambient surface. In addition to these two thermal boundary conditions, radiation effect was considered inside the cavity. This was defined by assuming the cavity faces as iso-thermal and iso-emissive surfaces.

Shahbazian and Wang [19] proposed simplified simulation methods to calculate the temperature distribution in the steel studs when the LSF panel is subjected to fire from one side. The 2-D FE models created in Abaqus consist of shell element type S4 with a mesh size of 2.5 mm. Abaqus FE simulation models were validated in two stages using previous test results. Experimental and numerical results obtained for one and two layers of gypsum plasterboards were compared in the first stage. In the second stage, the LSF wall configuration adopted in previous experimental studies was considered for finite element simulation using Abaqus. Comparison between the previous experimental studies and the proposed simulation results showed a good agreement with each other.

Nassif et al. [20] performed full scale fire tests of a non-load bearing LSF wall panel (3 m × 3 m) made of galvanised steel channel section studs (75 × 50 × 0.6 mm), two layers of 12.5 mm thick gypsum plasterboards on both sides of the wall and rock fibre cavity insulation. The wall panel was exposed to the standard ISO 834 fire curve. During their fire test, thermal

bowing and plasterboard fall-off were observed on the fire side at about 48 minutes. This was validated by a rapid rise in temperature between 48 and 50 minutes. Post-test inspections showed that the fire side plasterboard had fully lost the integrity. They proposed simplified methods to perform sequentially coupled thermal-mechanical analysis of their LSF wall system. At first a transient uncoupled thermal analysis was performed by considering only the thermal properties of LSF wall components and then a mechanical model was analysed without the plasterboards and insulation but considering their effect by including appropriate boundary conditions for plasterboards. Solid (DC3D8) and shell elements (S4) were used for uncoupled thermal and mechanical analyses, respectively. Although solid element provides good prediction in thermal simulations, it is not suitable for mechanical models because of the buckling effects of thin-walled stud elements. The FEA results were in good agreement with the measured temperature and deformation results from the experimental study until failure.

This brief literature review showed that the 3-D FE models of LSF wall systems have not been thoroughly investigated and the available literature is limited to only few test validations. Therefore, this research focuses on developing a 3-D FE model to investigate the fire performance of LSF wall systems, and then conduct a series of parametric studies using the developed FE model to better understand the behaviour of LSF wall systems with varying configurations.

3 3-D FE MODEL DEVELOPMENT

Fire performance of LSF wall systems has been widely investigated using full-scale fire tests and then compared with FEA results. Many research studies focused on developing a simplified numerical approach to simulate the test results. These simplified FEA were mainly based on 1-D and 2-D uncoupled FE models, which were developed with appropriate thermal-mechanical properties of LSF wall components such as wall board, cavity insulation and stud as well as boundary conditions such as convection and radiation.

Although these FEA results have provided a reasonable agreement with the full-scale fire test results, 3-D fully coupled thermal-mechanical FE models are needed to accurately simulate the fire behaviour of full scale wall panels. In comparison with 1-D and 2-D models, 3-D models will be more useful in simulating the effects of wall board configurations, cavity shapes, stud shapes, noggings, service holes in studs, partially fire exposed LSF walls and

different boundary conditions. These effects will develop non-uniform time-temperature profiles across the LSF wall during a fire event, thus 1-D or 2-D models are not suitable. Therefore, in this research a 3-D FE modelling approach was developed and validated with full-scale fire test results. The developed FE thermal models can be fully coupled to the structural modelling of the wall studs, which is an advantage of using the developed 3-D FE models. This section presents the details of the finite element (FE) thermal model development and validation using Gunalan et al.'s [15] fire test results for different LSF wall configurations lined with gypsum plasterboards and also with or without cavity insulation. These configurations were simulated using 3-D heat transfer models developed using Abaqus/CAE [17].

3.1 Thermal Properties of LSF Wall Components

3.1.1 Gypsum Plasterboard

An important aspect of thermal FE model development of LSF wall is the use of appropriate thermal properties for its components. Therefore, the measured thermal properties of gypsum plasterboard were used in the FE models with linear approximation to the measured properties. Such an approximation was adopted to avoid overloading the analysis with more data points and to reduce the analysis time. Keerthan and Mahendran [7] have conducted sensitivity analyses using measured and idealized thermal properties, which yielded similar FEA results.

The measured and proposed specific heat, thermal conductivity and density are shown Figures 1 to 3. Figure 1 shows the measured and proposed specific heat variation in gypsum plasterboard produced by Boral plasterboard [21]. Gypsum plasterboard exhibits two specific heat peaks of 17,500 and 13,500 J/kg/°C at 145 and 175 °C, respectively. This is mainly due to the dehydration of chemically bound water inside the gypsum plasterboard. Therefore, gypsum plasterboard will absorb heat and delay the temperature rise when exposed to fire at these temperatures.

Figure 2 shows the measured and proposed thermal conductivity of gypsum plasterboard. The measured thermal conductivity value of gypsum plasterboard at ambient temperature is approximately 0.2 W/m/ºC. This value reduces during the dehydration processes. However, after complete dehydration of water at about 200 ºC, the thermal conductivity increases due to the burning of paper on the outside skin of gypsum plasterboard, which is followed by

cracking at about 900 ºC with a sudden thermal conductivity increment. Therefore, appropriate thermal conductivity values were proposed in order to include the effect of ablation and cracking observed in gypsum plasterboard after the dehydration process. Figure 3 shows the relative density of gypsum plasterboard, which shows a mass loss of about 16% during the dehydration process. The original density of gypsum plasterboard used in this study was 781 kg/m^3. After this process, the relative density remains unchanged. Further discussions of these thermal properties can be found in Keerthan Mahendran [7].

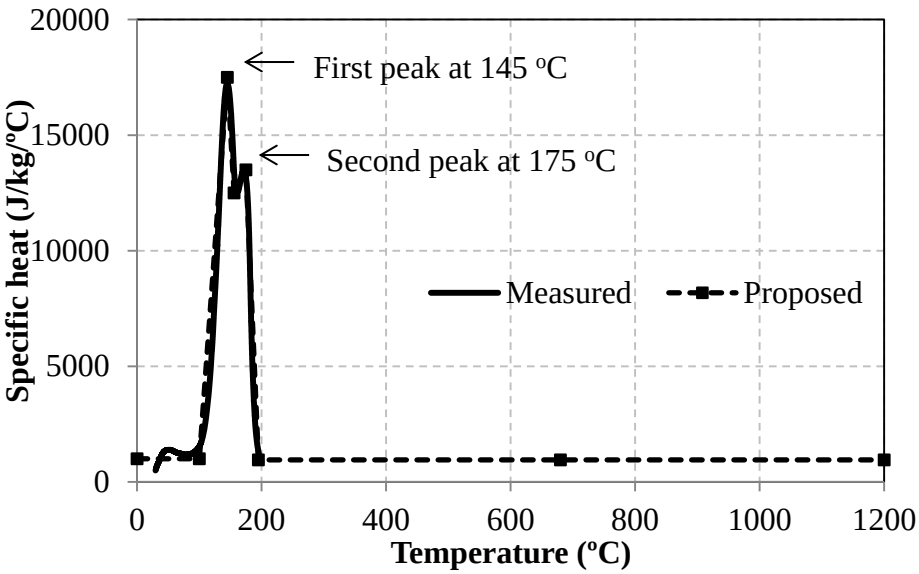

Figure 1. Specific heat of gypsum plasterboard

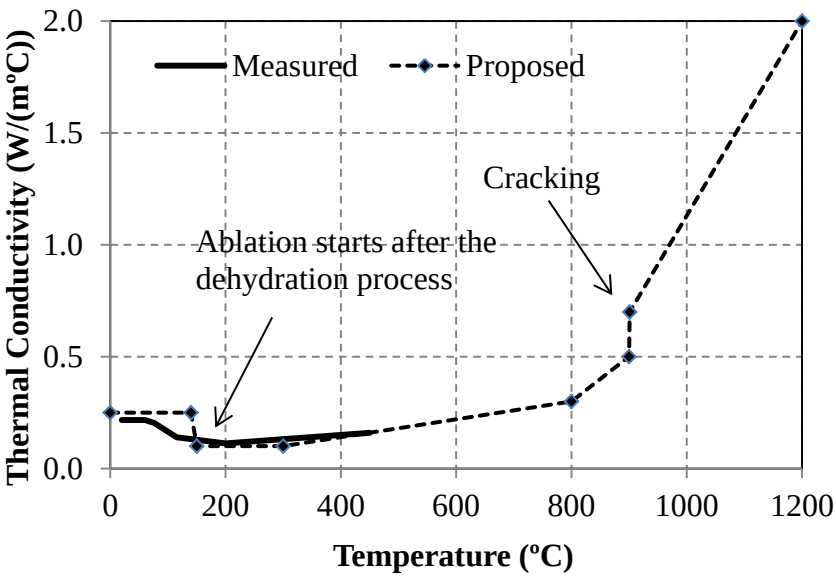

Figure 2. Thermal conductivity of gypsum plasterboard

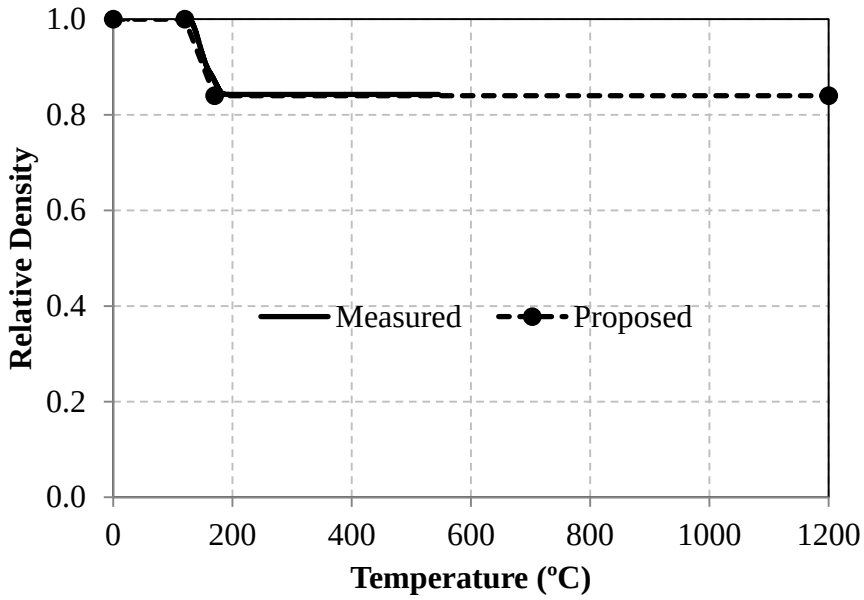

Figure 3. Relative density of gypsum plasterboard

3.1.2 Steel

Thermal properties of steel were obtained from Eurocode 3: Part 1-2 [22]. The specific heat and thermal conductivity profiles are shown in Figures 4 and 5. The density of the steel remains constant at 7,850 kg/m^3 at all temperatures.

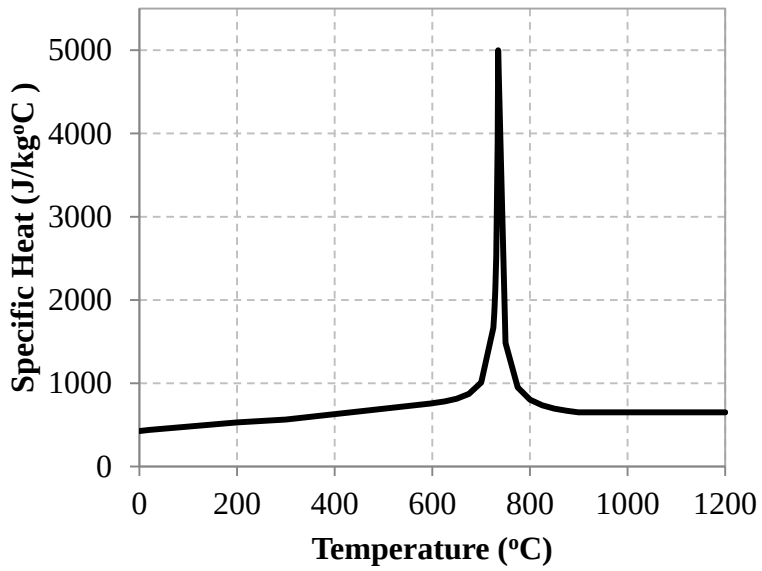

Figure 4. Specific heat of steel

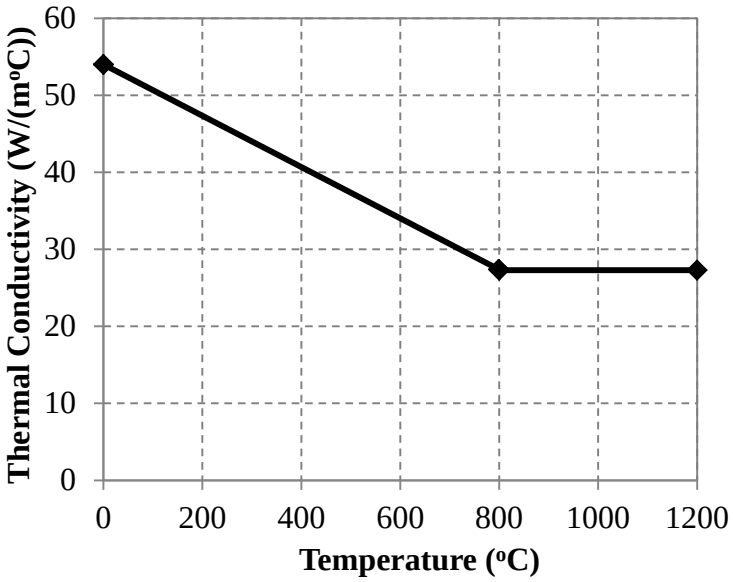

Figure 5. Thermal conductivity of steel

3.1.3 Insulation

Thermal properties of glass fibre, rock fibre and cellulose fibre insulation materials measured by Keerthan and Mahendran [7] were used in this study. They proposed constant specific heat values of 900, 840 and 1250 J/kg/ºC and density values of 15.42, 100 and 125 kg/m^3 for glass fibre, rock fibre and cellulose fibre insulation materials, respectively. However, the thermal conductivity values show a variation with temperature as shown in Figure 6. The sudden increase in glass fibre thermal conductivity is due to the melting of glass fibre at about 600-700 ºC as observed during fire tests performed by Gunalan et al. [15].

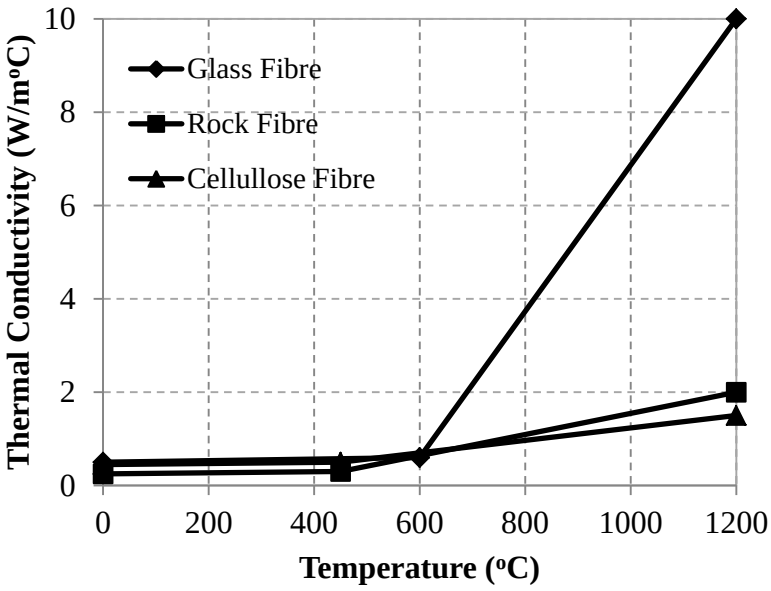

Figure 6. Thermal conductivity of insulation materials

3.2 Model Configurations

This section presents the details of FE model development and validation using Gunalan et al.'s [15] fire test results for LSF wall systems with five different configurations of 16 mm thick gypsum plasterboards and lipped channel studs (90×40×15×1.15 mm) spaced at 600 mm as listed in Table 1. The tests were conducted on 2.1 m × 2.4 m LSF walls exposed to standard fire curve on one side. The measured thermal properties of the wall components used in these fire tests are presented in the last section.

Table 1. LSF wall configurations tested by Gunalan et al. [15]

Model No.	*Configuration*	*Insulation*	*Board Configuration*	*Failure Time (minutes)*
1		None	Single board	54
2		None	Double boards	111
3		Glass Fibre	Double boards	101
4		Rock Fibre	Double boards	107
5		Cellulose Fibre	Double boards	110

3.3 FE Modelling Strategies

In the past, many research studies have focused on 2-D analysis of LSF wall systems due to less computing power and time required for 2-D analysis. Details of these analyses are discussed in the literature review of this paper. In contrast to 2-D analysis, the 3-D full-scale analysis of LSF wall system cannot be implemented by an average user using a normal computing system. However, with the currently available high performance computing (HPC) systems and advanced numerical analysis software such as Abaqus/CAE [17], full-scale 3-D analysis can be performed in considerably less time with high efficiency. This will improve the understanding of the behaviour of LSF walls exposed to fire as a whole system, which will enable the development of heat transfer and fully-coupled thermal-mechanical model. This research will focus on the heat transfer analysis of 3-D LSF wall systems.

The 3-D FE models representing the LSF wall configurations in Table 1 were developed in Abaqus/CAE [17], based on the two critical middle studs and gypsum plasterboards as shown in Figure 7. The overall dimensions of the model were 1.8 m × 2.4 m to represent the actual tested wall panels without considering the overhang of 150 mm on both sides. All the

LSF wall components were modelled using 8-node linear heat transfer brick elements (DC3D8). A mesh density of 50 mm on the x-y plane and 2 mm through thickness mesh of the gypsum plasterboard were selected based on a sensitivity analysis. Through thickness mesh is an important parameter, which decides the heat transfer through the thickness of gypsum plasterboard, thus a finer mesh was adopted in the z-direction.

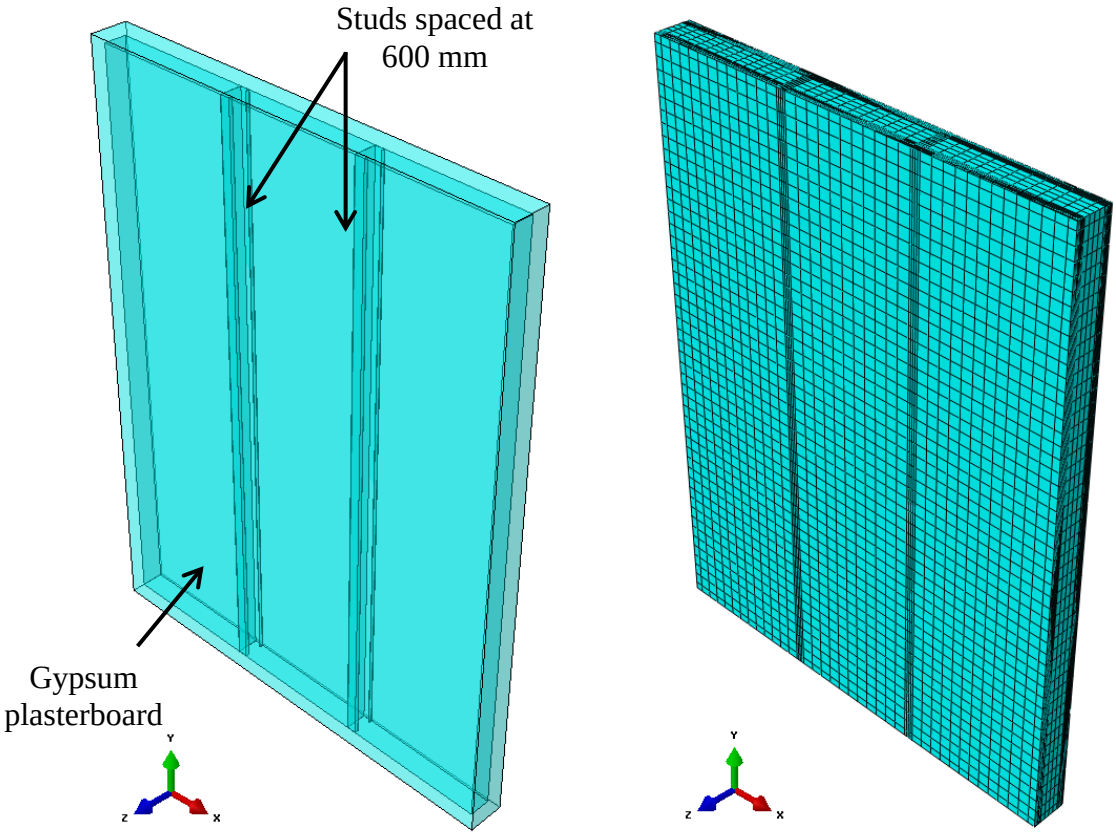

Figure 7. 3-D FE model of LSF wall (Model 2: LSF wall with double plasterboards)

3.4 Boundary Conditions

The LSF wall components were modelled using heat transfer solid elements (DC3D8) and then connected using tie constraints to ensure solid-solid heat transfer between them. There are three major heat transfer modes in FEA, namely; conduction, convection and radiation. The conduction effect was defined using appropriate conductivity values as discussed earlier in Section 3.1. The convection heat transfer was defined by assigning convective film coefficients of 25 and 10 W/m^2/^{o}C on the fire and ambient sides, respectively. These values were selected based on those proposed in the past research studies [7]. Finally, the radiation heat transfer was defined by assigning an emissivity value of 0.9 on all the LSF wall surfaces.

In addition to the above-discussed boundary conditions the studs were connected to the gypsum plasterboard using tie constraints to ensure heat transfer between the studs and the wall board without any gaps between them. In practice this is ensured by screwing the wall boards tightly to the studs. In some cases, the gap between the wall board and the steel stud need to be modelled using different elements to incorporate the joint separation that can occur due to different thermal properties of wall board and steel stud. The finite element analysis software has the option to model the interface element using thermal contact conductance or gap conductance properties. This research study did not consider this approach, thus the connection between the wall board and the steel studs was assumed to be connected throughout the fire exposure.

The models without interior cavity insulation materials were modelled in Abaqus/CAE using closed cavity radiation in enclosures. The cavity surfaces enclosed by the LSF wall components were selected first and then a cavity radiation emissivity of 0.9 was assigned to those surfaces. These boundary conditions are shown in Figure 8. The heat transfer through the LSF wall cavities without insulation occur predominantly by cavity radiation because the convective and conductive heat transfer through the air cavity is assumed to be negligible. As the air inside the confined cavity is motionless during LSF wall fire exposure, the convective heat transfer is considered negligible. On the other hand, conductive heat transfer through the cavity is also negligible due to very low thermal conductivity of the air inside the cavity.

Standard fire curve was defined as an amplitude curve following a time-temperature profile based on ISO 834, where $\theta = 345\log 10(8t + 1) + 20$, θ is the temperature and t is the time. This was assigned to the fire exposed side as nodal boundary condition. The temperature on the fire side was assigned to follow the fire curve, whereas a room temperature was assigned to the ambient side of gypsum plasterboards. The Stefan-Boltzmann constant (σ) of 5.67×10^{-8} W/m^2/ºC^4 was also assigned to the model.

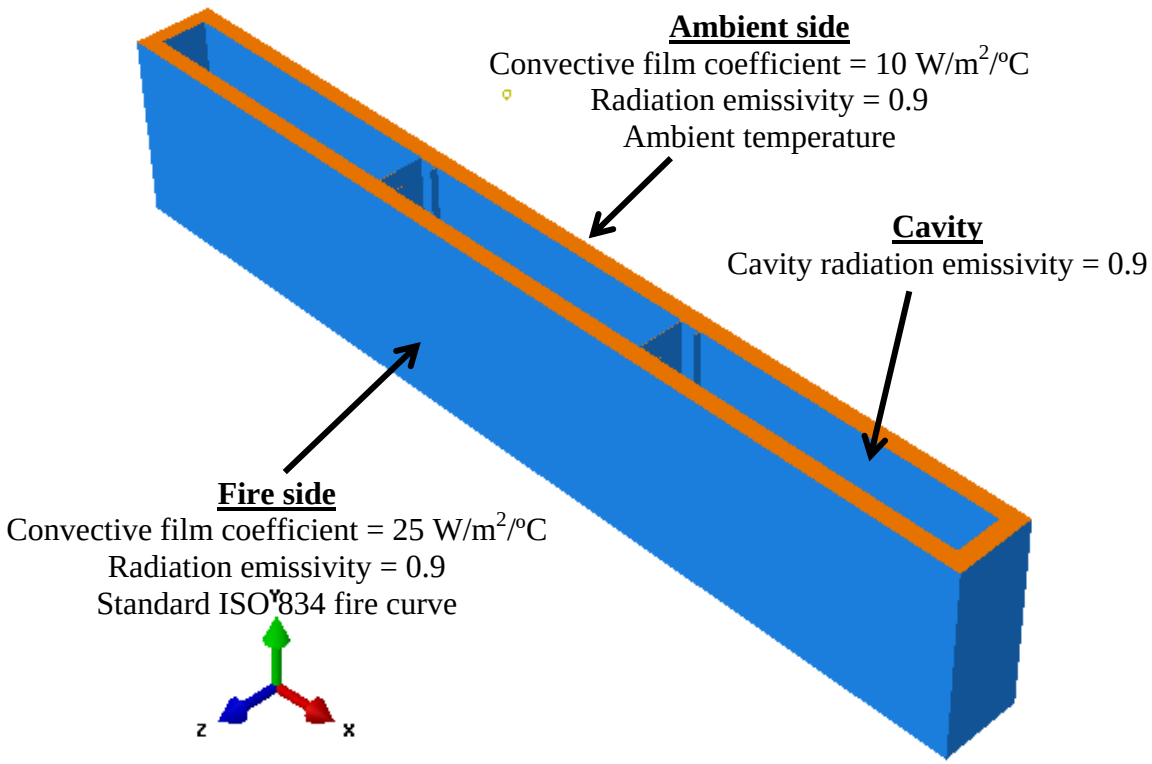

Figure 8. Boundary conditions assigned to the FE Model 2

4 FE MODEL VALIDATION OF TESTED LSF WALL SYSTEMS

The 3-D FE models were analysed until the LSF wall failure times reported by Gunalan et al. [15], which are given in Table 1. Temperature contours obtained from the FEA for Model-2 are shown in Figure 9. The experimental average time-temperature profiles (hot flange - HF, web and cold flange - CF) of the middle two studs are compared with the FEA results in Figures 10 (a) to (e). In addition, the average time-temperature profiles measured on the plasterboards at different surfaces of the wall as shown in Figure 9a (Fire side – Fire, Fire side cavity surface – Fire-In, Ambient side cavity surface – Amb-In, Ambient side – Amb) are also compared with the FEA results in Figures 11 (a) to (e). The experimental and FEA results show a very good agreement for all five LSF wall configurations. The 3-D heat transfer FE models were able to capture the transient temperature profiles with good accuracy, and most importantly, the hot flange temperature values were predicted with good accuracy at failure. The failure times in the fire tests of LSF wall configurations 1 to 5 were 54, 111, 101, 107 and 110 minutes, respectively (refer Table 1). Therefore, these validated FE models can be used to accomplish further investigations of different wall configurations. It is to be noted that the developed model does not include the effect of moisture movement in the board during fire exposure.

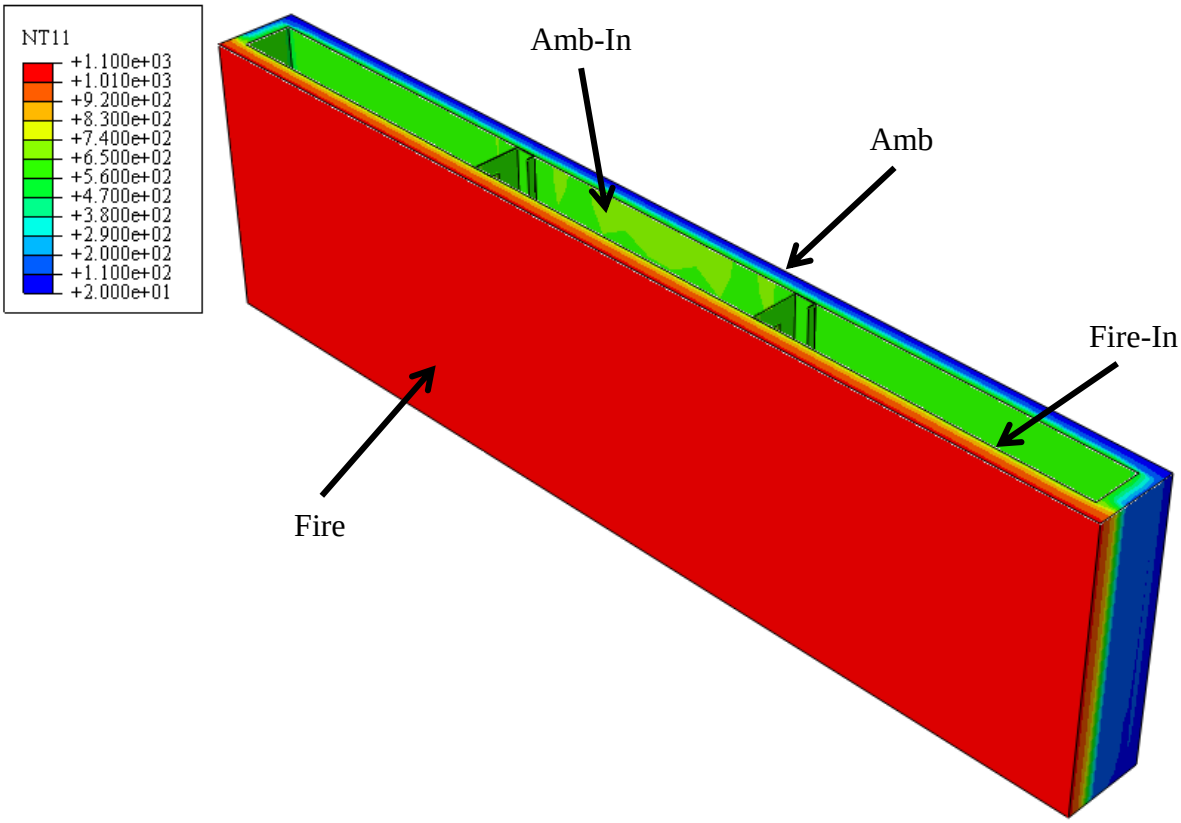

(a) Model temperature contours at 120 minutes

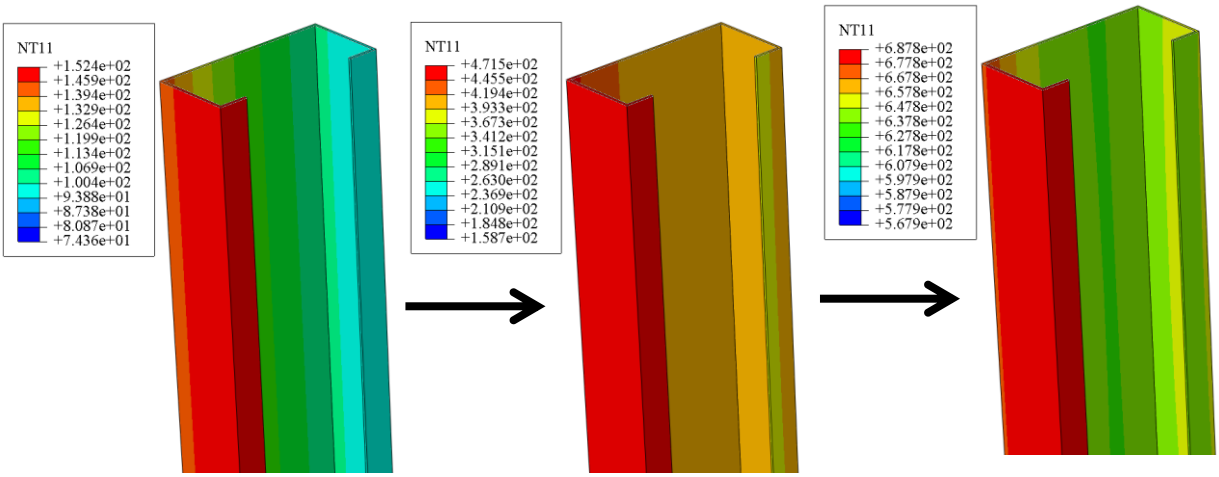

(b) Stud temperature contours at 60, 90 and 120 minutes

Figure 9. Temperature contours of Model 2 (Double plasterboard lined LSF wall)

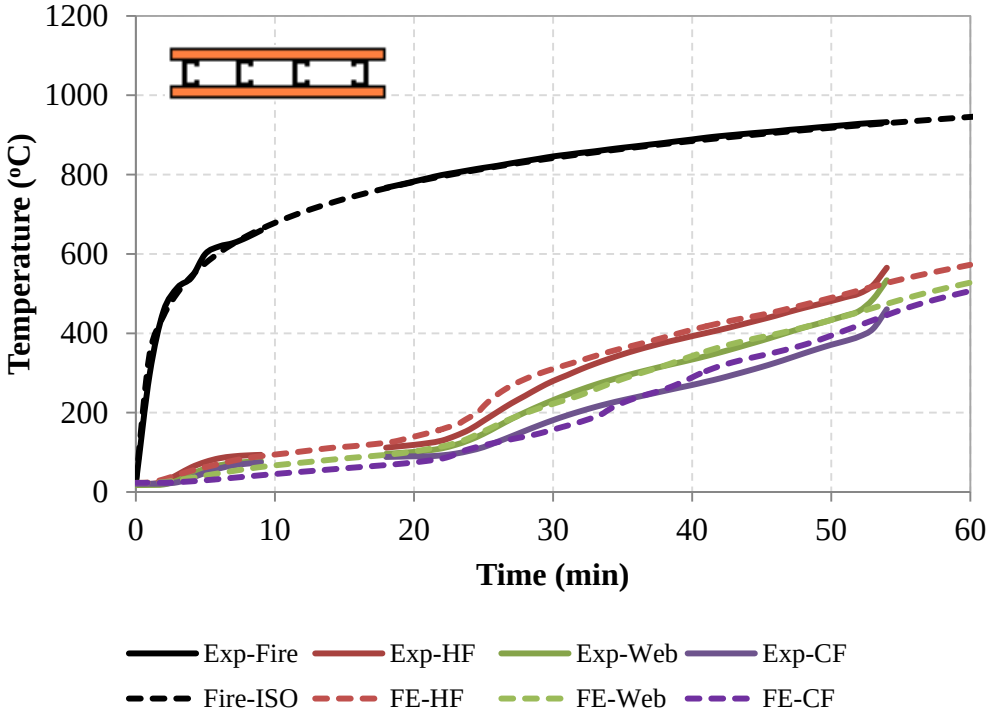

(a) Model 1

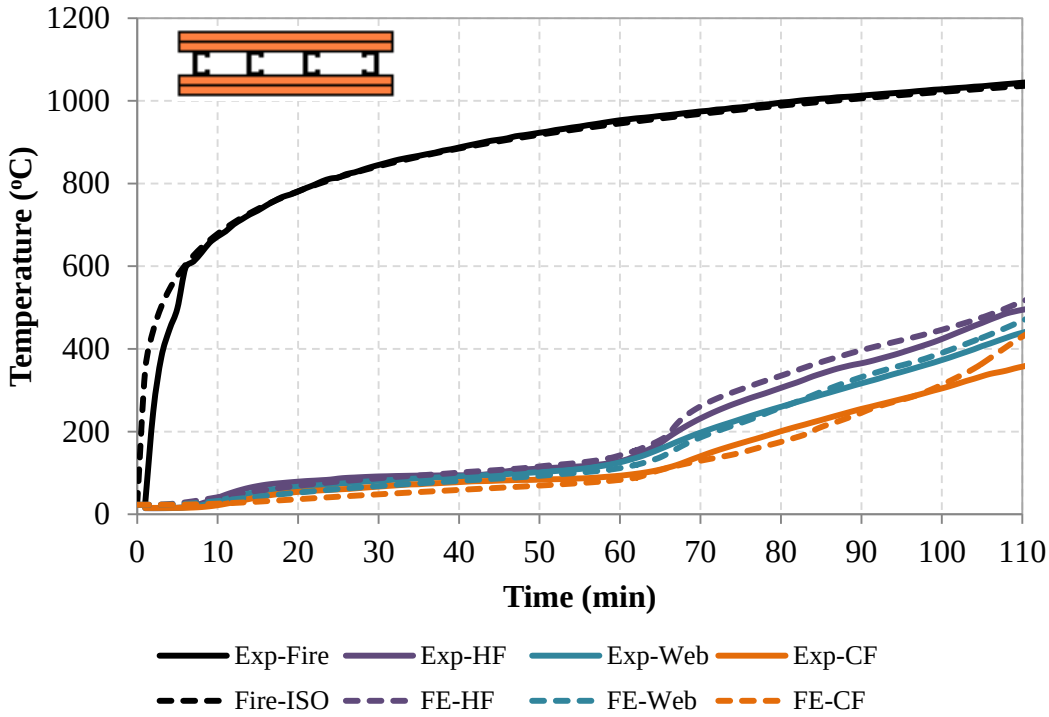

(b) Model 2

Figure 10. Stud time-temperature profiles

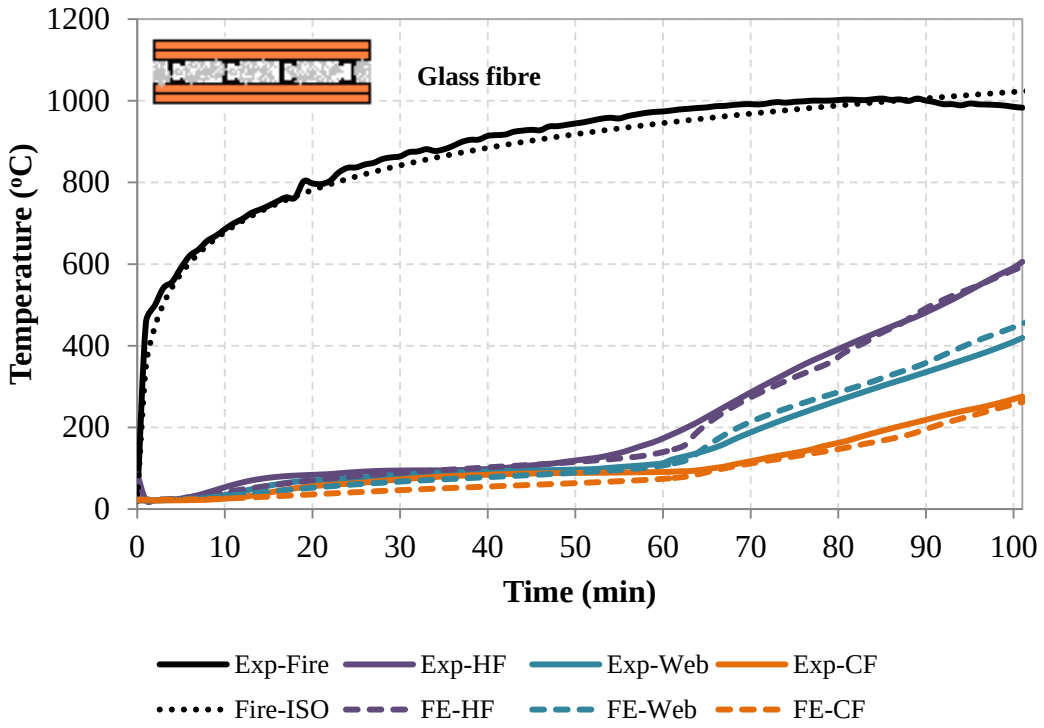

(c) Model 3

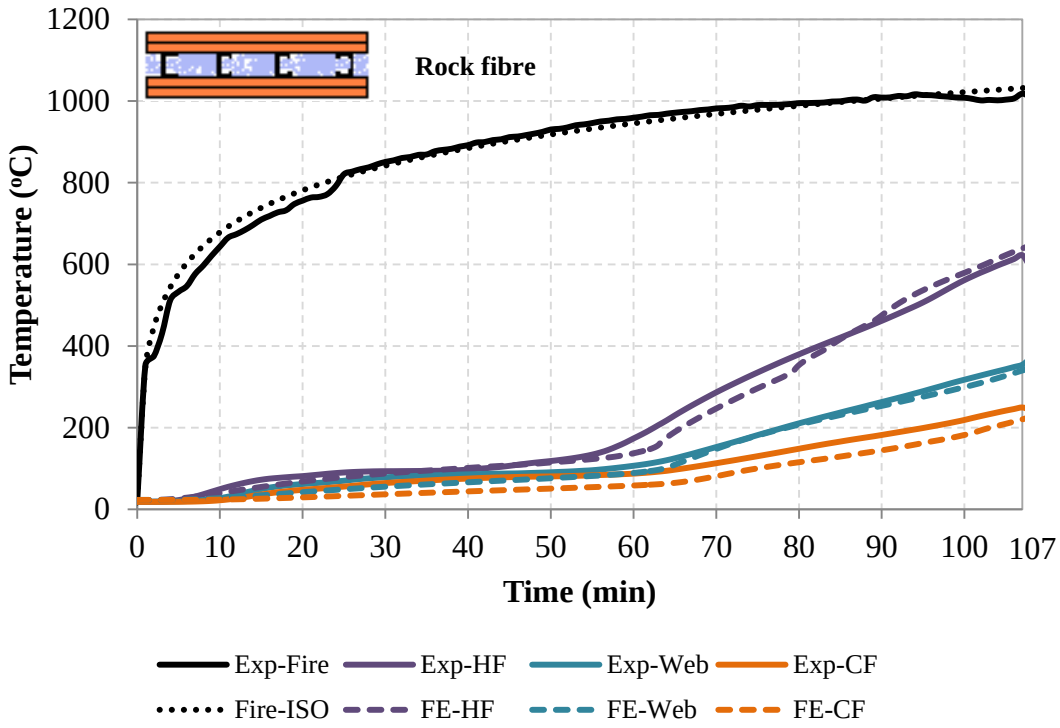

(d) Model 4

Figure 10. Stud time-temperature profiles

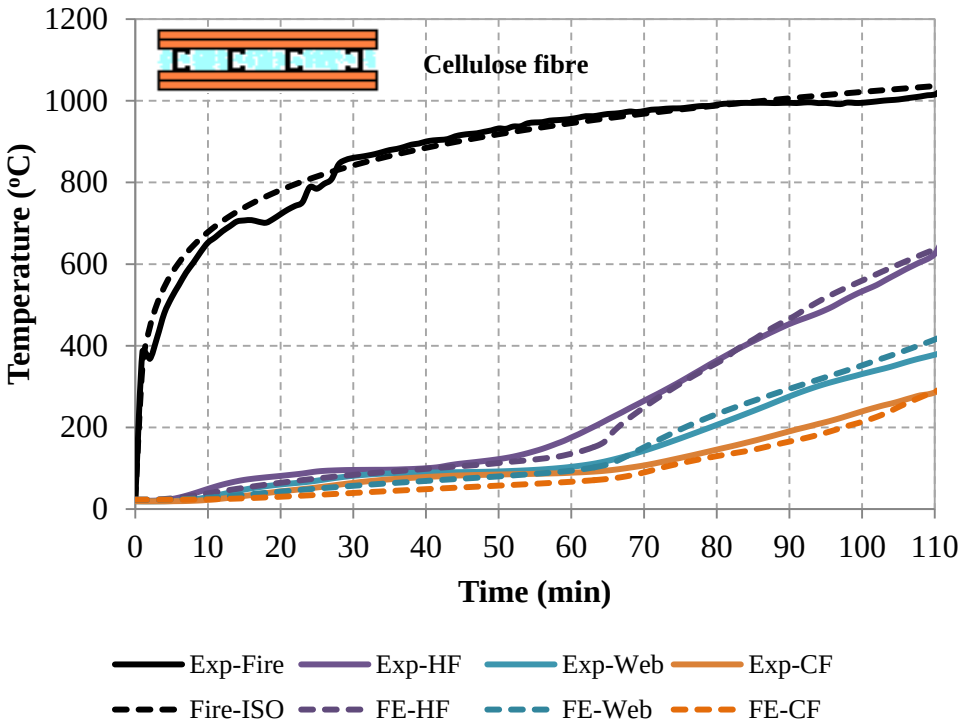

(e) Model 5

Figure 10. Stud time-temperature profiles

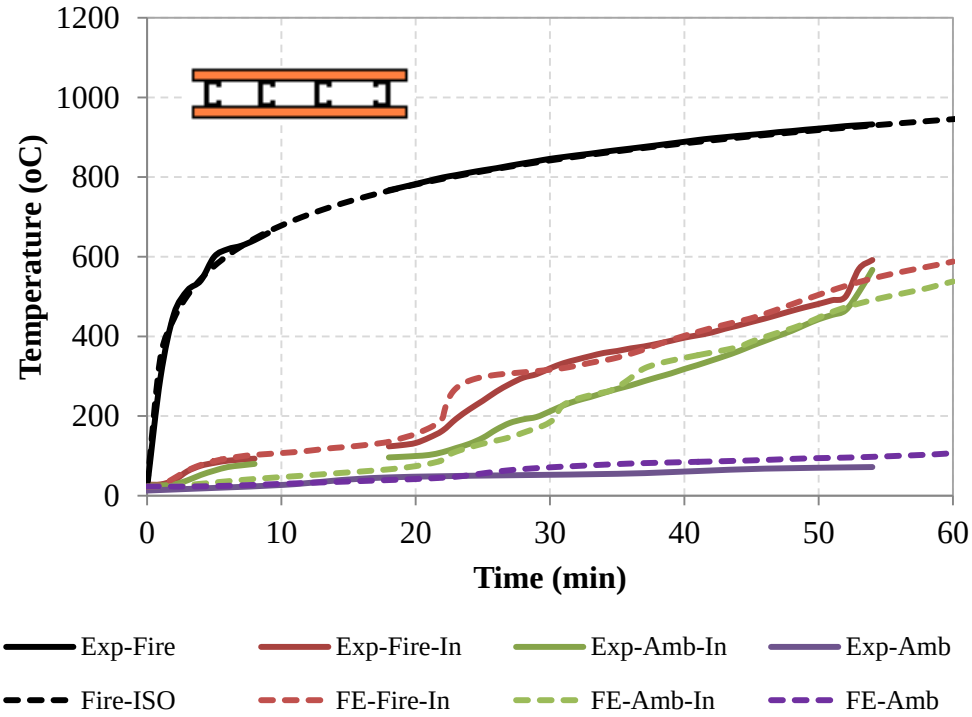

(a) Model 1

Figure 11. Plasterboard time-temperature profiles

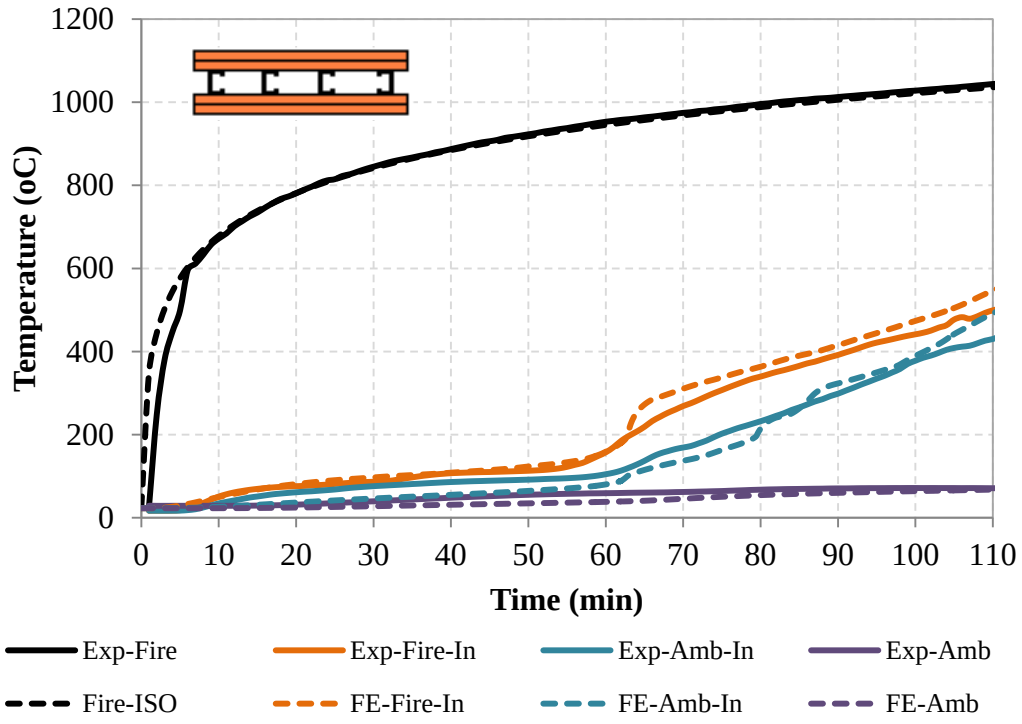

(b) Model 2

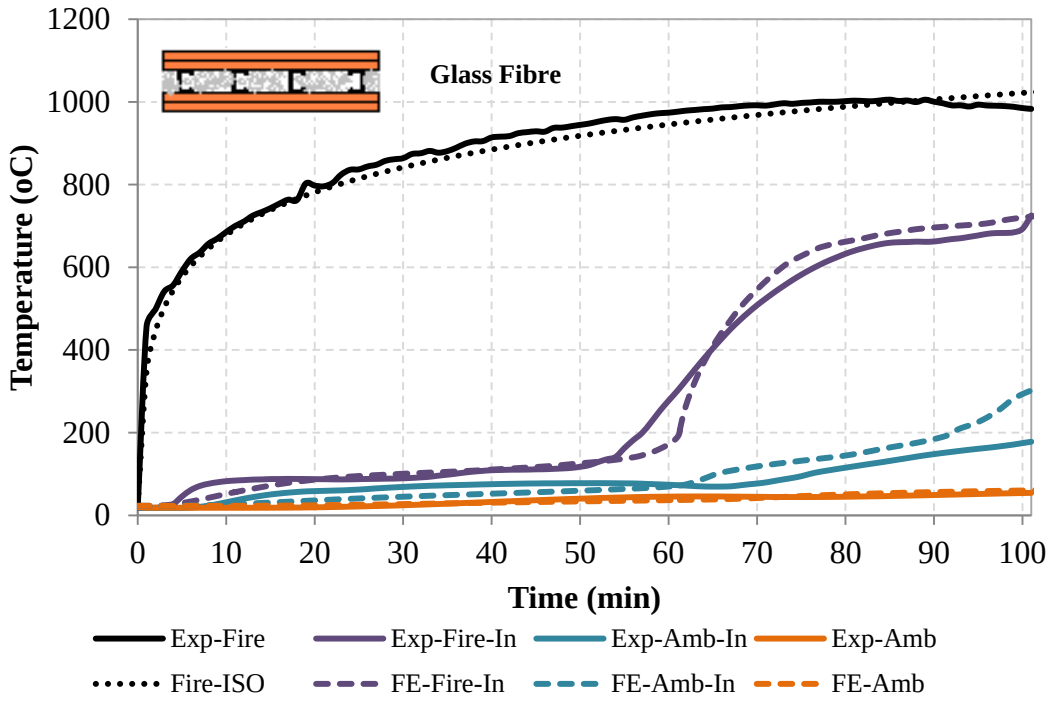

(c) Model 3

Figure 11. Plasterboard time-temperature profiles

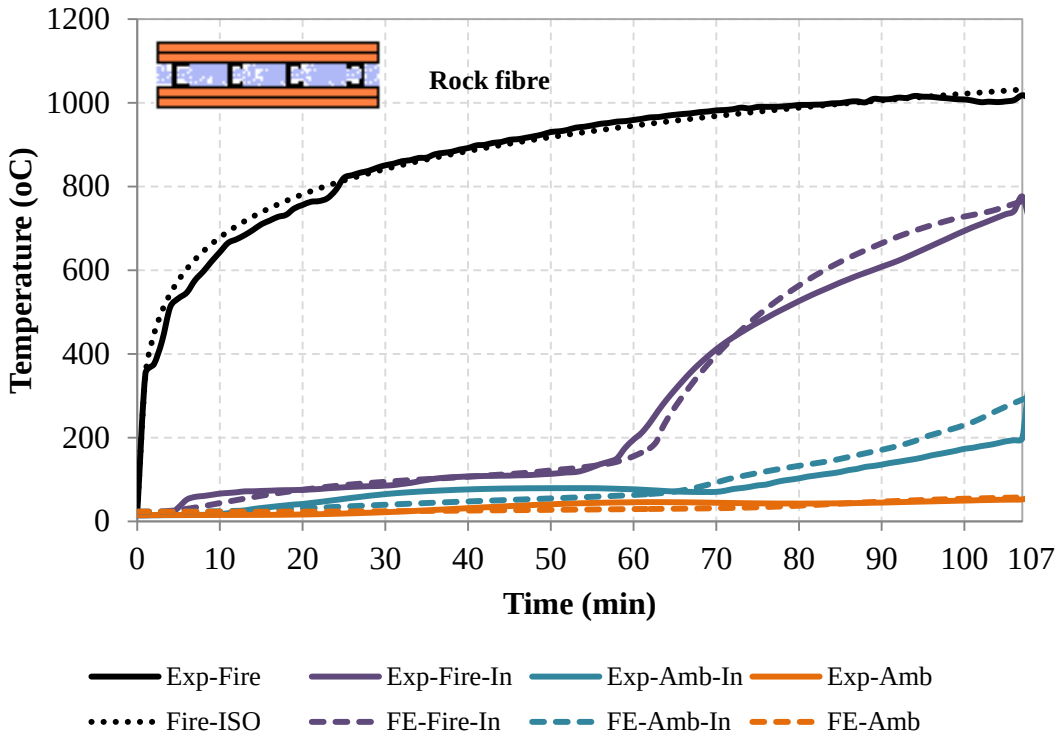

(d) Model 4

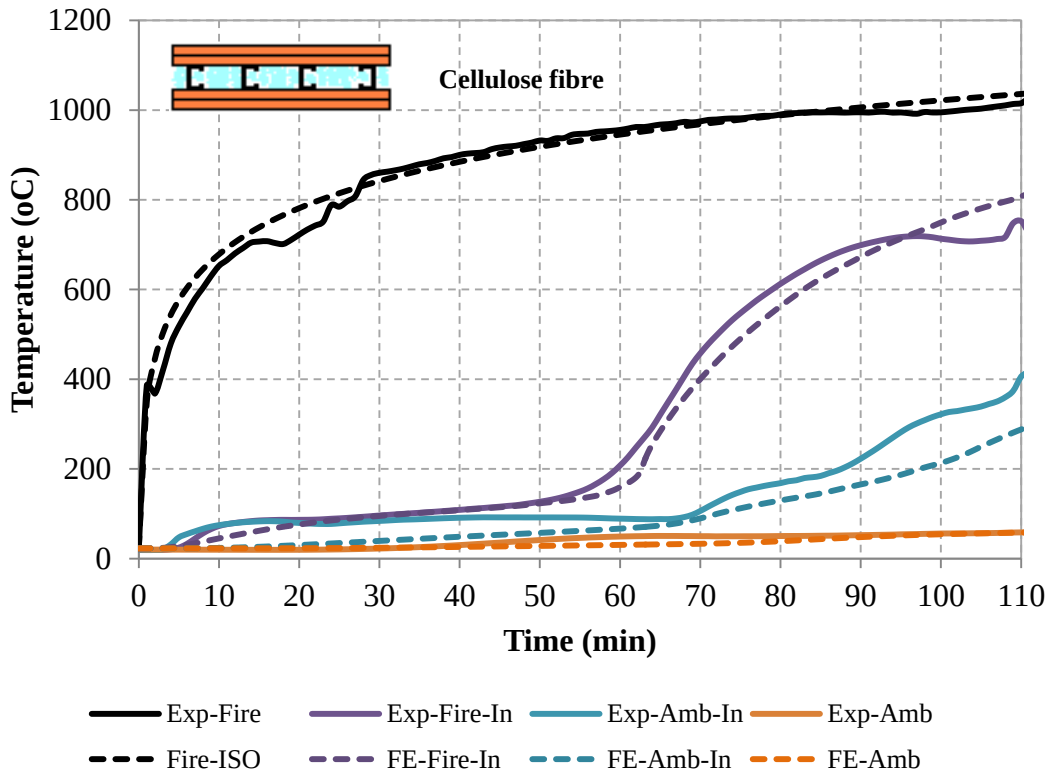

(e) Model 5

Figure 11. Plasterboard time-temperature profiles

5 PARAMETRIC STUDY OF LSF WALL SYSTEMS WITH DIFFERENT CONFIGURATIONS

Typical LSF wall systems are made of cold-formed steel frames, gypsum plasterboard and cavity insulation. These components are vulnerable under fire exposure due to deterioration of mechanical properties at elevated temperatures and temperature dependent thermal properties. When there is fire on one side of the LSF wall, the plasterboards and cavity insulation keep the temperatures of the studs and the wall boards on the unexposed side well below their failure temperatures for a longer period of time. These failure times are defined as fire resistance levels (FRLs).

The most commonly used LSF wall configurations are made of cold-formed light-gauge steel frame lined with single layer of gypsum plasterboard on both sides. When the plasterboard joint is constructed over the steel stud, this LSF wall configuration has limited FRL due to premature joint failure during the fire exposure, which leads to rapid increase in the stud temperature along the joints. This type of premature joint failure can be eliminated by adding more plasterboard layers and staggering the plasterboard joints. However, this indirectly increases the weight and cost of the wall systems.

Another method to protect the steel studs from reaching failure temperatures is to place a back-blocking over the steel stud behind the gypsum plasterboard joints. In practice these back-blockings are 150 mm wide and made of similar materials as wall lining board. The effect of having a back-blocking along plasterboard joints over the steel stud is discussed in this section. On the other hand, most of the LSF wall component manufacturers recommend the use of cavity insulation to enhance the thermal comfort of the building. However, the effect of having cavity insulation compared to no cavity insulation has not been fully investigated. Therefore, this section also compares the failure times of different LSF wall configurations with and without cavity insulation.

5.1 Model Configurations

A parametric study was conducted on six different LSF wall configurations (Table 2) using the validated 3-D finite element (FE) modelling strategies discussed earlier in this paper. LSF wall configurations lined with single and double gypsum plasterboard layers, and with and without cavity insulation were analysed (Models A, B, E and F). In addition, the LSF wall systems with a 150 mm wide back-blocking made of gypsum plasterboard over the

steel studs were also analysed (Models C and D). During construction the back-blocking is screw fastened first to the studs and then the outer wall board layer is screw fastened to the studs through back-blocking. In the FE model the back-blocking was considered to be fully connected to the studs and the wall board through tie constraints. The 3-D FE models of 1.8 m × 2.4 m were developed for these LSF wall configurations with 16 mm thick gypsum plasterboard layers and two lipped channel studs (90×40×15×1.15 mm) spaced at 600 mm with and without rock wool cavity insulation (Figure 12). The parametric study models were developed with the same material properties and boundary conditions discussed in Section 3 and were exposed to the standard ISO 834 fire curve on one side.

Table 2. LSF wall configurations used in the parametric study

Model No.	*Configuration*	*Insulation*	*Board Configuration*
A		None	Single board
B	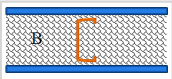	Rock Fibre	Single board
C	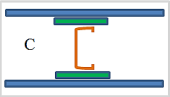	None	Single board with 150 mm wide back-blocking
D	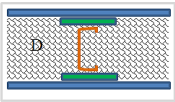	Rock Fibre	Single board with 150 mm wide back-blocking
E		None	Two boards
F	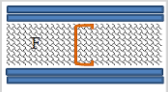	Rock Fibre	Two boards

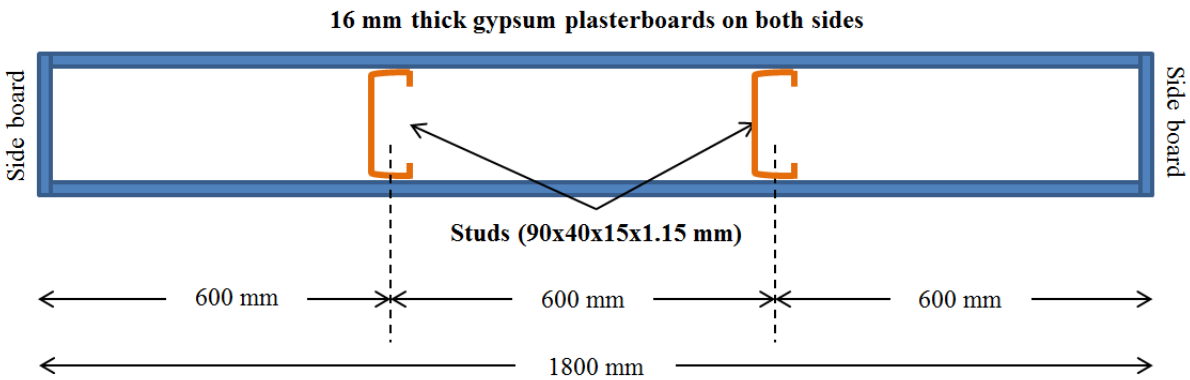

Figure 12. Schematic of LSF wall configuration of Model A

5.2 FEA Results

The time-temperature profiles of the hot flange (HF) and the ambient surface of the wall board are shown in Figures 13 and 14. In Figure 13, the FEA results were obtained until all the models have reached a maximum hot flange temperature of 600 ºC, which was proven as the approximate failure temperature of most of the load bearing cold-formed steel studs at a load ratio of 0.2 [2]. The steel stud hot flange temperature variation shows a unique feature between similar models with and without cavity insulation, in which they tend to follow the same profile up to a certain temperature and then deviates from each other. As an example, Models A and B with and without cavity insulations are compared, both models follow the same time-temperature profiles up to about 25 minutes of fire exposure and then deviates from each other. The hot flange temperature at this point is approximately 200 ºC. This time is about 60 and 80 minutes for Models C, D and Models E and F, respectively, and the hot flange temperature is about 300 and 350 ºC, respectively.

After this point, the temperature of the LSF wall configurations with cavity insulation (Models B and F) significantly increased at a rapid rate compared to a slow increase in temperature of uninsulated LSF wall configurations (Models A and E). Therefore, it can be concluded that the cavity insulation does not have any effects on load bearing walls (LBWs) up to a certain hot flange (HF) temperature, and after this point, the uninsulated LBWs will perform better than cavity insulated walls. The temperatures on both insulated and uninsulated LBWs are unaffected until the gypsum plasterboard on the fire side is fully dehydrated and become softer. After this point the heat transmits through the gypsum plasterboard rapidly to the cavity. During this period the cavity insulated walls absorb more heat compared to uninsulated walls, so that the cavity materials act as heated body and thus the hot flange temperature is increased quicker than in uninsulated air filled cavity walls.

This trend was not observed in models with back-blocking in Models C and D. A small deviation was observed in the opposite direction where the cavity insulated wall (Model D) performed better than the uninsulated wall (Model C). This is because the wall configurations in Models C and D were modelled with a 150 mm wide back-blocking, in which the width of the board affects the hot flange temperatures. Therefore, different back-blocking widths may produce varying hot flange temperatures. In addition to these observations, the LSF wall configurations with back-blocking (Model C and D) performed better than the single layer

gypsum plasterboard configurations in Models A and B, in which the temperature increase in the studs was further delayed by the back-blocking.

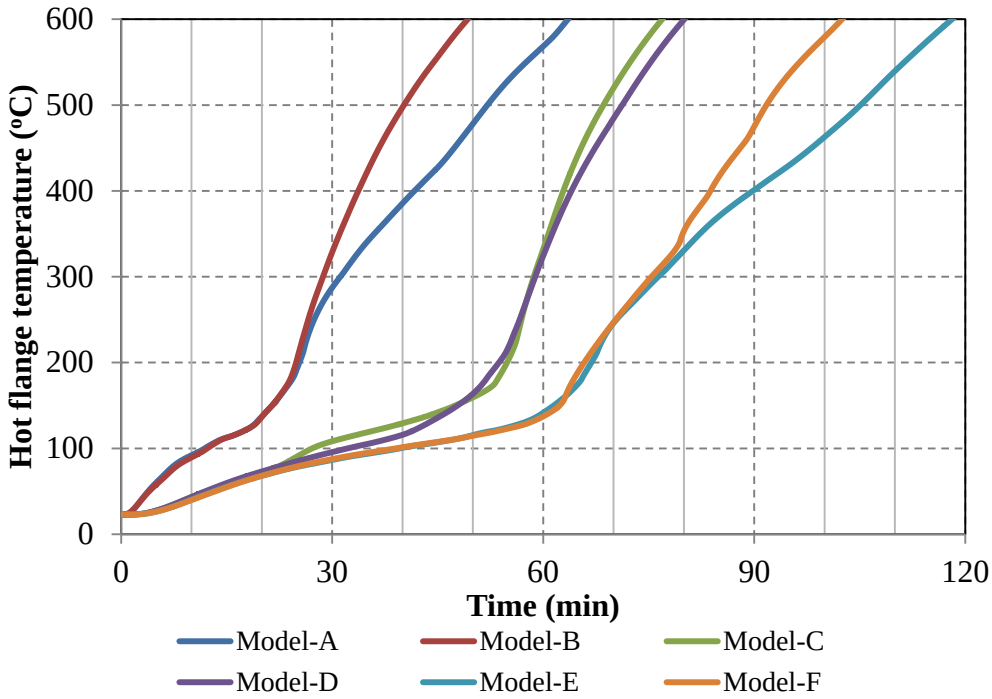

Figure 13. Steel stud hot flange temperature variation for structural failure criterion

The time-temperature profiles on the ambient surface of LSF walls for Models A to F are shown in Figure 14. The analysis results were plotted to a maximum temperature of 200 ºC, which is assumed to be the failure temperature of a non-load bearing wall (NLBW) under insulation failure criterion as described earlier and the analyses were conducted up to 300 min (5 hours) of fire exposure.

Figure 14 shows that the failure times of NLBWs are significantly delayed when cavity insulation is used. For example, the difference between cavity insulated and uninsulated single plasterboard Models A and B is about 40 minutes. This difference is about 90 minutes for Models C and D and 105 minutes for Models E and F, respectively. This is a significant improvement in failure times of NLBWs. Therefore, it can be concluded that NLBWs will significantly benefit from cavity insulation when exposed to fire in addition to the enhanced thermal comfort.

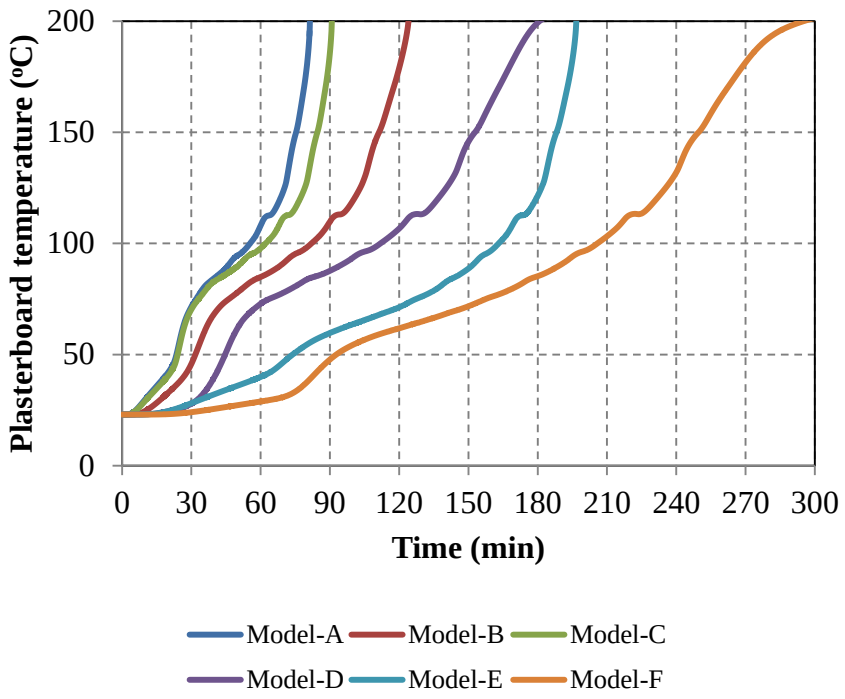

Figure 14. Ambient side plasterboard temperature variation for insulation failure

5.3 Failure Time Comparison for LSF Walls with Different Configurations

As stated earlier the failure temperatures of load bearing walls (LBWs) are mainly dependent on the hot flange temperatures of the steel stud. The hot flange temperatures for different load bearing LSF wall configurations vary with the load ratios (LR), where the LR is defined as the ratio between the applied load and the ultimate failure load. Gunalan and Mahendran [2] performed experimental and numerical analyses of different LSF wall configurations and developed a set of load ratio versus hot flange temperature curves. Based on their results, similar studs will fail at the same hot flange temperature at a given load ratio. Therefore, the steel stud failure temperature of a LBW for the respective load ratios will be; 1) LR=0.2: 600 ºC, 2) LR=0.4: 500 ºC, 3) LR=0.6: 300 ºC and 4) LR=0.7: 200 ºC. It is noted that the failure temperatures reduce when the load ratio is increased. These findings were also observed during experimental studies and FEA performed on gypsum plasterboard lined lipped channel stud LSF walls by Gunalan et al. [15] and Ariyanayagam and Mahendran [16].

This approach was adopted in this study to obtain the failure times in the parametric analysis of LBW configurations. For non-load bearing walls (NLBW), the failure times were calculated based on the assumption that the failure occurs under insulation failure criterion, in which the temperature on the unexposed or ambient side surface of the LSF wall reaches a

maximum temperature of 200 ºC during the analysis. Table 3 lists the failure times obtained from the FEA for NLBWs and LBWs with varying load ratios. As seen in Table 3 the failure times of LBWs are significantly reduced with increasing load ratios.

Table 3. Failure times from the parametric study

	NLBW	*LBW*			
Configuration		*LR=0.2 (600 ºC)*	*LR=0.4 (500 ºC)*	*LR=0.6 (300 ºC)*	*LR=0.7 (200 ºC)*
A	80	60	50	30	25
B	120	50	40	30	25
C	90	75	70	60	55
D	180	80	70	60	55
E	195	120	105	75	65
F	300	100	90	75	65

5.4 Comparison and Discussion

The failure times in Table 3 were compared for all six LSF wall configurations considered in this study to better understand the effect of cavity insulation and the back-blocking. The failure times of NLBWs are shown in Figure 15 and LBWs with different load ratios from 0.2 to 0.6 are shown in Figures 16 and 17. The load ratio of 0.6 (failure temperature of 300 ºC) is the most commonly adopted load ratio in load bearing walls.

5.4.1 Non-Load Bearing Wall Assemblies

Figure 15 illustrates the importance of having cavity insulation for non-load bearing walls such as internal or partition walls in a building. The failure time of single layer gypsum plasterboard configuration is improved by 40 minutes in Model B compared to Model A when cavity insulation is used. This failure time improvement is much higher when two layers of gypsum plasterboard are used (Model E vs Model F). Although the configuration with back-blocking without cavity insulation (Model C) does not improve the failure time compared to Model A, the back-blocking with cavity insulation Model D has a 60 minutes failure time improvement compared to Model B. Therefore it can be concluded that back-blocking has a significant effect on NLBW assemblies when they are cavity insulated. On the other hand, the most effective NLBW configuration is the double layer gypsum plasterboard with cavity insulation, which provided a failure time of more than 240 minutes.

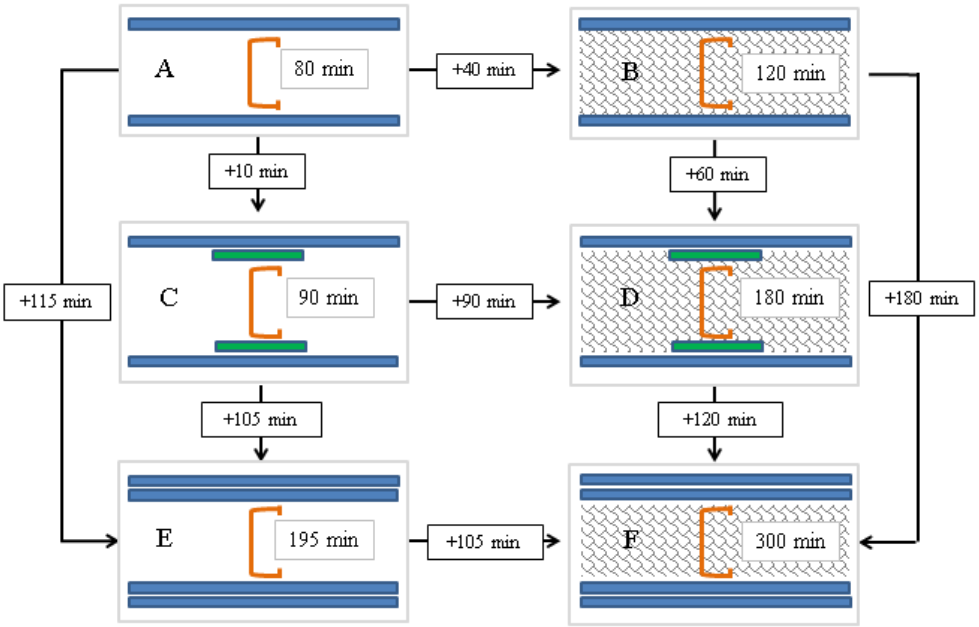

Figure 15. Insulation failure time comparison for NLBW

5.4.2 Load Bearing Wall Assemblies with LR=0.2

The steel stud's hot flange failure temperature is 600 ºC for a load ratio of 0.2. The failure times of six load bearing LSF wall configurations are shown in Figure 16, which shows the detrimental effect of cavity insulation for lower load ratios. When cavity insulation is used, the failure times of LBWs with single layer (Models A and B) and two layers (Models E and F) are reduced by 10 and 20 minutes, respectively. This reduction is due to the heating of cavity insulation materials, which eventually acts as a heat source inside the cavity.

However, this reduction was not observed in the LSF wall configurations with back-blocking in Models C and D, which has an improvement of 5 minutes in cavity insulated wall configuration. This is mainly due to the back-blocking protecting the steel from being heated up to a certain extent. However, when Model B and D are compared, the failure time is improved by 30 minutes when back-blocking is used, in which the same configuration has been used with increased cavity width. However, different back-blocking widths and thicknesses may result in varying failure times. Apart from this particular configuration with back-blocking, it can be concluded that cavity insulation significantly reduce the failure times of LSF wall systems lined with single and two gypsum plasterboard subjected to lower load ratios.

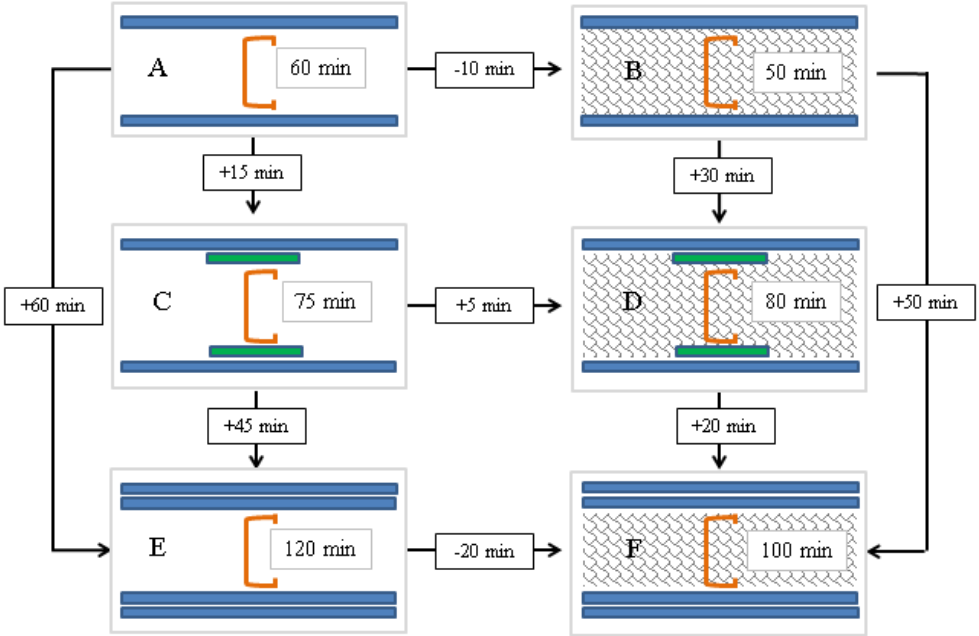

Figure 16. Structural failure time comparison for LBW with LR=0.2 (600 ºC)

5.4.3 Load Bearing Wall Assemblies with LR=0.6

The steel stud's hot flange failure temperature is 300 ºC for a load ratio of 0.6. Figure 17 compares the failure times of different load bearing LSF wall assemblies with a load ratio of 0.6. This comparison shows a unique feature in the failure times of uninsulated and insulated LSF wall configurations. When the load ratio is about 0.6, the failure times are not affected by the inclusion of cavity insulation, thus both cavity insulated and uninsulated LSF wall configurations provide the same failure times (Models A, C and E compared to Models B, D and F).

This is mainly due to the fact that the gypsum plasterboard does not dehydrate completely and become soft until reaching 300 ºC. Therefore, the temperature increase inside the cavity is not affected significantly. This phenomenon can also be observed in LSF walls with a load ratio of 0.7. In addition, it is observed that the use of back-blocking in Models C and D improves the failure times by 30 minutes compared to LSF walls lined with single layer of gypsum plasterboard (Models A and B).

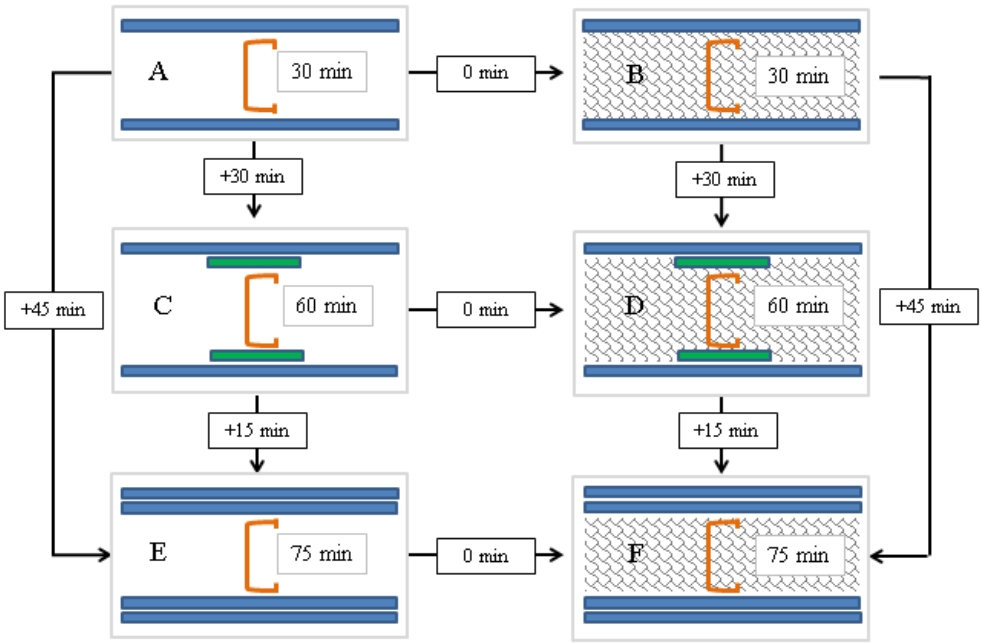

Figure 17. Structural failure time comparison for LBW with LR=0.6 (300 ºC)

5.4.4 Summary

In summary, Figure 18 presents the FRLs of the six LSF wall configurations considered in the parametric study based on the failure times obtained from FEA. The Building Code of Australia [23] requires a minimum FRL of 60/60/60 minutes for most commonly used buildings. Based on the parametric FEA, the LSF wall configurations lined with two layers of gypsum plasterboard with or without cavity insulation in Models E and F are capable of meeting the minimum requirement for all cases of NLBW and LBW.

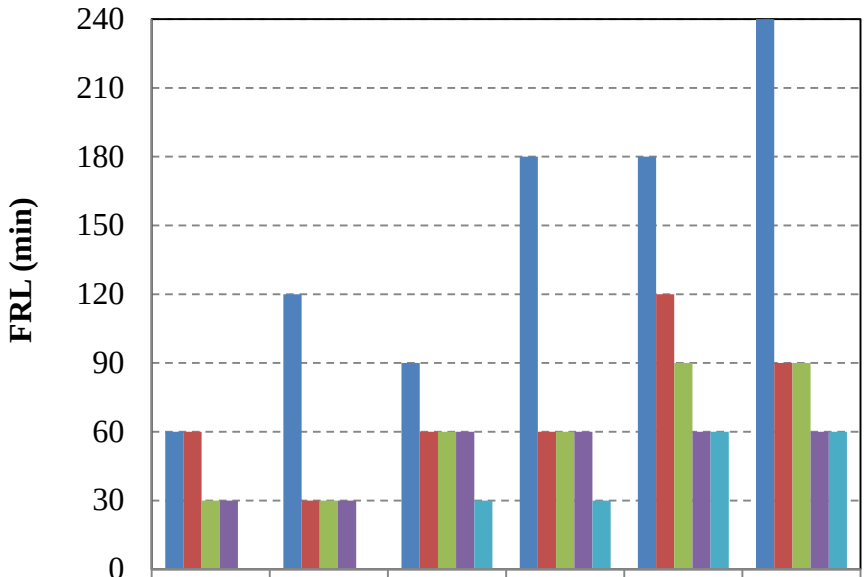

	A	B	C	D	E	F
NLBW	60	120	90	180	180	240
LR=0.2 (600 °C)	60	30	60	60	120	90
LR=0.4 (500 °C)	30	30	60	60	90	90
LR=0.6 (300 °C)	30	30	60	60	60	60
LR=0.7 (200 °C)	0	0	30	30	60	60

Figure 18. Fire resistance levels (FRLs) of different LSF wall configurations

6 CONCLUSIONS

This paper has presented the details of 3-D FE model development strategies used in this research and the validation of 3-D FEA results using the measured time-temperature profiles in an experimental study of five different LSF wall configurations. These 3-D FE models were developed using solid elements while appropriate thermal properties and boundary conditions were used by incorporating measured data. A good agreement was observed between the experimental and FEA stud and plasterboard transient time-temperature profiles. These validated 3-D FE models were then utilized to conduct a parametric study of different LSF wall configurations. The following conclusions can be made from this study.

- These 3-D FE models can be used to conduct parametric studies of various LSF wall configurations based on different types of boards, cavity insulation and stud sections. Using the 3-D FE models developed in this research, a direct coupling of the heat transfer analysis can be made to the thermal-mechanical modelling of the studs to include the non-uniform temperature variation along the height and across the stud. This method can be used to develop a fully-coupled FE model to investigate thermal-mechanical behaviour of LSF wall systems simultaneously.
- Steel studs can be protected by back-blocking, which enhances the fire performance of the walls by keeping the stud temperatures below relevant failure limits. However, this in turn slightly increases the cavity depth. The use of back-blocking significantly improves the failure times of the wall systems lined with single layer gypsum plasterboard. It is recommended to further investigate the effects of different back-blocking widths and thicknesses on the failure times of LSF wall systems.
- The failure times of cavity insulated LSF walls subjected to load ratios less than 0.4 are less than those of the uninsulated LSF walls. This is due to the complete dehydration of the fire side wall boards and heating of cavity insulation materials that eventually act as a heat source, which decreases the failure time of cavity insulated LSF walls. When the load ratio is higher than 0.6, the failure times are not affected by the cavity insulation materials.

ACKNOWLEDGEMENTS

The authors would like to thank Queensland University of Technology (QUT) for providing the necessary research facilities, and Australian Research Council (ARC) and QUT for providing the financial support to conduct this research project.

REFERENCES

[1] S. Kesawan, M. Mahendran, Fire tests of load-bearing LSF walls made of hollow flange channel sections. Journal of Constructional Steel Research, 115 (2015), December 2015, pp. 191-205.

[2] S. Gunalan, M. Mahendran, Fire performance of cold-formed steel wall panels and prediction of their fire resistance rating. Fire Safety Journal, 64 (2014), pp. 61-80.

[3] W. Chen, J. Ye, Y. Bai, X.L. Zhao, Full-scale fire experiments on load-bearing cold-formed steel walls lined with different panels. Journal of Constructional Steel Research, 79 (2012), pp. 242-254.

[4] W. Chen, J. Ye, Y. Bai, X.L. Zhao, Improved fire resistant performance of load bearing cold-formed steel interior and exterior wall systems. Thin-Walled Structures, 73 (2013), pp. 145-157.

[5] J.M. Franssen, SAFIR – A Thermal/Structural program modelling structures under fire. Engineering Journal, 42 (2005), pp. 143-158.

[6] G. Thomas, Modelling thermal performance of gypsum plasterboard-lined light timber frame walls using SAFIR and TASEF. Fire and Materials, 34 (2010), pp. 385-406.

[7] P. Keerthan, M. Mahendran, Thermal performance of composite panels under fire conditions using numerical studies: plasterboards, rockwool, glass fibre and cellulose insulations. Fire Technology, 49 (2) (2012), pp. 329-356.

[8] S. Kesawan, M. Mahendran, Predicting the performance of LSF walls made of hollow flange channel sections in fire. Thin-Walled Structures, 98 (A), (2016), pp. 111-126.

[9] V. Jatheeshan, M. Mahendran, Numerical Study of LSF Floors Made of Hollow Flange Channels in Fire. Journal of Constructional Steel Research, 115 (2015), pp. 236–251.

[10] Standards Australia (SA), AS 1530.4: 2005, Methods for fire tests on building materials, components and structures, Part 4: Fire-resistance tests of elements of building construction, 2005, Sydney, Australia.

[11] V. Jatheeshan, M. Mahendran, Experimental study of LSF floors made of hollow flange channel section joists under fire conditions. Journal of Structural Engineering, ASCE, 142 (2) (2016), 040215134.

[12] M.A. Sultan, V.R. Kodur, Light-weight frame wall assemblies: Parameters for considering in fire resistance performance-based design. Fire Technology, 36 (2) (2000), pp. 75-82.

[13] P. Keerthan, M. Mahendran, R.L. Frost, Fire safety of steel wall systems using enhanced plasterboards. Proceedings of the International Council for Research and Innovation in Building and Construction (CIB) World Building Congress 2013, 5-9 May, 2013, Brisbane, Australia.

[14] P. Kolarkar, M. Mahendran, Experimental studies of gypsum plasterboard and composite panels under fire conditions. Fire and Materials, 38 (2012), pp. 13-35.

[15] S. Gunalan, P. Kolarkar, M. Mahendran, Experimental study of load bearing cold-formed steel wall systems under fire conditions. Thin-Walled Structures, 65 (2013), pp. 72-92.

[16] A. Ariyanayagam, M. Mahendran, M. Experimental study of load-bearing cold-formed steel walls exposed to realistic design fires. Journal of Structural Fire Engineering, 5 (4) (2014), pp. 291-330.

[17] Dassault Systems Simulia Corp., Providence, RI, USA. Abaqus/CAE User's Guide, 2015.

[18] M. Feng, Y.C. Wang, J. Davies, Thermal performance of cold-formed thin-walled steel panel systems in fire. Fire safety journal, 38 (4) (2003), pp. 365-394.

[19] A. Shahbazian, Y.C. Wang, A simplified approach for calculating temperatures in axially loaded cold-formed thin-walled steel studs in wall panel assemblies exposed to fire from one side. Thin-Walled Structures, 64 (2013), pp. 60-72.

[20] A.Y. Nassif, I. Yoshitake, A. Allam, Full-scale fire testing and numerical modelling of the transient thermo-mechanical behaviour of steel-stud gypsum board partition walls. Construction and Building Materials, 59 (2014), pp. 51-61.

[21] Boral Plasterboard Ltd. Product Manual, Sydney, Australia, 2014.

[22] EN 1993-1-2: 2005, Eurocode 3: Design of steel structures. Part 1-2: General Rules - Structural Fire Design, European Committee for Standardization, Brussels, 2005.

[23] National Construction Code (NCC) Series, 2015, Building Code of Australia.